0 (0000) 0 – 0

Please leave this space empty

Progressive Fracture of $[0/90/\pm\theta]_S$ Composite Structure Under Uniform Pressure Load

Pascalis K. Gotsis[1*], Christos C. Chamis[2], Christos K. Gotsis[3], and Ericos Mouratidis[1]

[1]Dept. of Mechanical Engineering, Technological Educational Institute, Serres
Terma Magnisias, Serres, 62124, Greece
(pkgotsis@teiser.gr and emour@teiser.gr)

[2]NASA Glenn Research Center, Cleveland, Ohio 44135
(Christos.C.Chamis@grc.nasa.gov)

[3]Chemistry Dept., Aristotle's University, Thessaloniki, Greece.
(gotsis@chem.auth.gr)

Abstract

S-Glass/epoxy $[0/90/\pm\theta]_S$ for θ=45°, 60° and 75° laminated fiber-reinforced composite stiffened plate was simulated to investigated for damage and fracture progression under uniform pressure. An integrated computer code was augmented for the simulation of the damage initiation, growth, accumulation, and propagation to fracture and to structural collapse.

Results show in detail the damage progression sequence and structural fracture resistance during different degradation stages. Damage through the thickness of the laminate initiated first at $[0/90/\pm 45]_S$ at 15.168 MPa (2200 psi), followed by $[0/90/\pm 60]_S$ at 16.96 MPa (2460 psi) and finally by $[0/90/\pm 75]_S$ at 19.3 MPa (2800 psi). After damage initiation happened the cracks propagate rapidly to structural fracture.

Keywords: Laminates, composites, stiffened panel, simulation, fracture, degradation, failure, collapse load

1. Introduction

The aircraft, marine and automotive industries use stiffened composite plates because of their low weight, high stiffness, and stability. Design considerations with regard to the durability stiffened plates require a priori evaluation of the damage initiation and propagation mechanisms under expected service loads. Concerns of the safety and survivability of critical components require quantifications of the composite structural damage tolerance during overloads. Characteristic flexibilities in the tailoring of composite structures make them more versatile for fulfilling structural design requirements. However, these same design flexibilities render the assessment of composite structural response and durability more complex, prolonging the design and certification process and adding to the cost of the final product. It is difficult to evaluate composite structures because of the complexities in predicting their overall congruity and performance, especially when

* Corresponding Author
Manuscript received August 3, 2006

structural degradation and damage propagation occur. The prediction of damage initiation, damage growth, and propagation to fracture are important in evaluating the load-carrying capacity, damage tolerance, safety, and reliability of composite structures. The most effective way to obtain this quantification is through integrated computer codes that couple composite mechanics with structural analysis and damage progression models. GENOA computer code was used in this study. The code is an updated and improved version of CODSTRAN computer code [1]. The simulation of progressive fracture has been verified to be in reasonable agreement with the experimental data, such as damage progression in carbon fiber reinforced plastic I-beams [2] and carbon/carbon composite plate specimen subjected to three-point bending [3]. A variety of composite structures have been used to simulate the damage progression such as: stiffened adhesively bonded composite structures [4], damage progression in bolted composite structures [5], damage tolerance of composite pressurized thin shell structures [6], and progressive fracture of laminated fiber-reinforced composite stiffened plate under mechanical and thermo-mechanical loads [7] to [9].

The purpose of this paper is to perform computational simulation of a S-Glass/epoxy $[0/90/\pm\theta]_S$ for $\theta = 45°$, 60°, and 75° laminated reinforced-fibers composite stiffened plate, subjected to pressure load.

2. Methodology

The computational simulation is performed by coupling three modules: (1) composite mechanics, (2) finite element analysis, and (3) damage progression tracking. The damage progression module relies on the composite mechanics code ICAN [10] for composite micromechanics, macromechanics and laminate analysis, and calls a finite element analysis module that uses anisotropic thick shell elements to model laminated fiber-reinforced composite structures. The finite element module is based on the mixed finite element method [11]. By supplying the boundary conditions, the type of analysis desired, the applied loads, and the laminate properties, the module performs the structural analysis. In addition the finite element module provides the computed stress resultants to composite mechanics module, which continuously computes the developed ply stresses for each ply and checks for ply failure.

A computational simulation cycle begins with the definition of constituent properties from a material databank. Composite ply properties are computed by the composite mechanics module. The composite mechanics module also computes through-the-thickness structural properties of each laminate. The finite element analysis module accepts the composite properties that are computed by the composite mechanics module at each node and performs the analysis for a load increment. After an incremental finite element analysis, the computed generalized nodal force resultants and deformations are supplied to the composite mechanics module that evaluates the nature and amount of local damage, if any, in the plies of the composite laminate. Individual ply failure modes are determined using failure criteria associated with a) the negative and positive limits of the six ply stresses components (the in plane stresses ($\sigma_{l11}, \sigma_{l12}, \sigma_{l22}$) and the interlaminar stresses ($\sigma_{l33}, \sigma_{l13}, \sigma_{l23}$)), b) a modified distortion energy (MDE) combined stress failure criterion, and c) interply delamination due to relative rotation of the plies.

The generalized stress-strain relationship for each node is revised according to the composite damage evaluated by the composite mechanics module after each finite element analysis. The model is automatically updated with a new finite element mesh and properties, and the structure is reanalyzed for further deformation and damage. If ply failure criteria indicate new or additional damage during a load increment, the damage tracking module degrades the composite properties affected by the damage and reanalyzes the structure under the same load. When there is no indication of further damage under a load, the structure is considered to be in equilibrium. Subsequently, another load increment is applied leading to possible damage growth, accumulation, or propagation. In the computational simulation cases presented in this paper, analysis is stopped when commencement of the damage propagation phase is indicated by laminate fracture. Laminate fracture is predicted when major principal failure criteria are met for all plies at all nodes. After laminate fracturing, the composite structure is anticipated to enter a final damage propagation stage that leads to ultimate structural fracture or collapse.

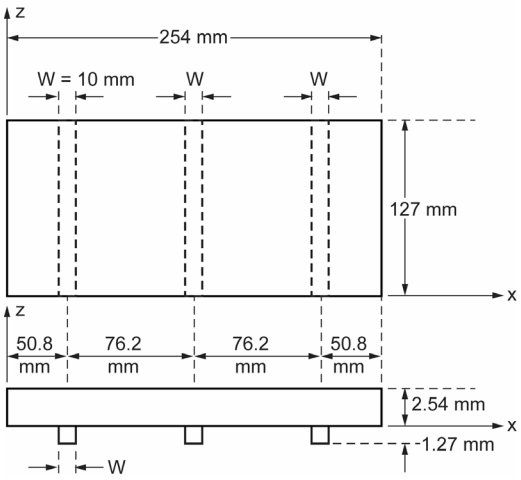

Figure 1. A laminated fiber–reinforced composite stiffened plate.

3. Fiber Composite Structures

The composite structure used for this investigation is a stiffened plate, figure 1. The length of the stiffened plate is 254 mm (10 in.) and the width is 127 mm (5 in.). The constituent properties for the fiber are listed in table 1 and for the matrix in table 2. The plate and the stiffened bands are made of S-Glass fibers and high strength (IMHS) epoxy matrix. Three different laminate configurations $[0/90/\pm\theta]_S$ for θ = 45°, 60°, and 75° were examined separately. The fiber volume ratio is 0.60. The skin laminate of the panel consists of eight 0.3175 mm (0.0125 in.) plies, resulting in a composite thickness of 2.54 mm (0.10 in.). The stiffened bands well bonded to the bottom surface of the panel with ply thickness equal to 0.1587 mm (0.00625 in.) resulting in a total thickness equal to 1.27 mm (0.05 in.). The 0° plies are in the X-axis (fig. 1), the first ply lays at the bottom surface of the plate, while the last ply lies at the top surface of the plate. The boundary conditions are fixed supported in all edges.

The finite element mesh consists of 396 elements and 442 nodes. Thick shell element was used for the computational simulation.

4. Results and Discussion

Damage initiation and progression were monitored as the panel was gradually loaded with the pressure. The damage progression of the stiffened plate as a function of the applied load is shown in figure 2. In our studies damage is defined as the volume of the damaged plies divided by the total volume of the structure.

Table 1. S-Glass Fiber Properties

Number of fibers per end	200
Fiber diameter, mm (in.)	0.00762 (0.3×10^{-3})
Normal modulus, GPa (psi)	
Longitudinal	85.5 (12.4×10^{6})
Transverse	85.5 (12.4×10^{6})
Poisson's ratio	
ν_{12}	0.20
ν_{23}	0.20
Shear modulus, GPa (psi)	
G_{12}	35.67 (5.17×10^{6})
G_{23}	35.67 (5.17×10^{6})
Thermal expansion coefficient, /°C (/°F)	
Longitudinal	0.509×10^{-5} (0.280×10^{-5})
Transverse	0.509×10^{-5} (0.280×10^{-5})
Heat conductivity, J-m/hr/m^2/ °C (Btu-in./hr/in.^{2}/°F)	
Longitudinal	(5.208×10^{-2})
Transverse	(5.208×10^{-2})
Heat capacity, J/Kg/°C (Btu/lb/°F)	712 (0.17)
Strength, MPa (Ksi)	
Tensile	2482 (360)
Compressive	2068.33 (300)

Table 2. IMHS Epoxy Matrix Properties

Matrix density, Kg/m^3 (lb/in.^{3})	3×10^{-7} (0.0443)
Normal modulus, GPa (ksi)	3.394 (500)
Poisson's ration	0.35
Coefficient of thermal expansion, /°C (°F)	0.7704 (0.428×10^{-4})
Heat conductivity, J-m/hr/m^2/°C (Btu-in./hr/in.^{2}/°F)	(8.680E–03)
Heat capacity, J/Kg/ °C (Btu/lb/ °F)	738 (0.250)
Strength, MPa (Ksi)	
Tensile	103.41 (15.)
Compressive	241.3 (35.)
Shear	89.62 (13.)
Allowable strain	
Tensile	0.02
Compressive	0.05
Shear	0.045
Torsional	0.045
Void conductivity, J-m/hr/m^2/°C (Btu-in./hr/in.^{2}/°F)	16.8 (0.225)
Glass transition temperature, °C (°F)	216 (420)

4.1 Damage initiation

At the damage initiation stage, all damaged plies of the $[0/90/\pm\theta]_S$, θ = 45°, 60°, and 75° subjected to matrix cracking due to tensile transverse failure mode of the 0° plies (bottom and top).

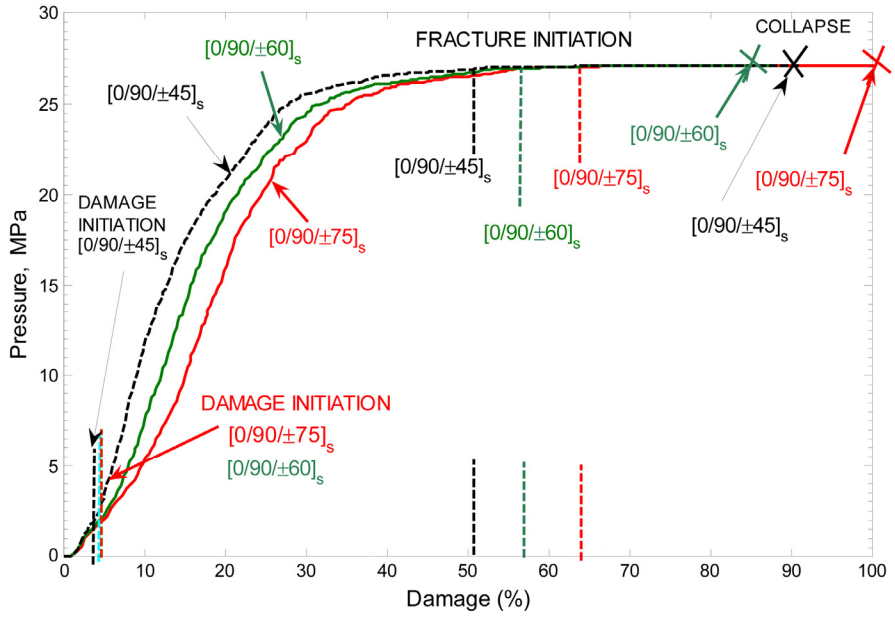

Figure 2. Damage progression under pressure S-Glass/Epoxy stiffened plate. Comparison of the laminate configurations $[0/90/\pm\theta]_S$ for $\theta = 45°$, 60°, and 75°.

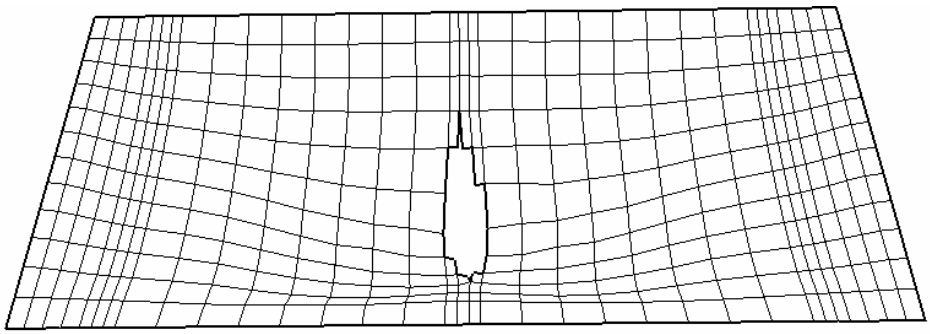

Figure 3(a). Fracture initiation at $P = 15.17$ MPa (2200 psi) [0/90/±45]s S-Glass/Epoxy Stiffened plate.

The damage initiation started first at the $[0/90/\pm45]_S$ at 0.41 MPa (60 psi), figure 2.
Almost 16.7 percent of the damaged plies failed due to fiber breaking (bottom (0°) ply) due to the longitudinal compressive failure mode.
Laminate $[0/90/\pm\theta]_S$ for $\theta = 60°$ and 75° the damage initiation started at| 0.552 MPa (80 psi), figure 2. Laminate $[0/90/\pm60]_S$ 30 percent of the damaged plies had fiber fracture at the bottom (0°) ply and 30 percent interply delamination at the top (0°) ply. Laminate $[0/90/\pm75]_S$, 33 percent of the damaged plies had fiber fracture due to the longitudinal compressive failure mode at the bottom (0°) ply and the same percentage had interply delamination due to the relative rotation criterion at the top (0°) ply.

4.2 Damage initiation through the thickness of the laminate

Increasing the load, the damages spread extensively and propagated through the thickness of the laminate, figure 2. Damage initiated first at $[0/90/45/-45]_S$ at 15.168 MPa (2200 psi), followed by $[0/90/\pm60]_S$ at 16.96 MPa (2460 psi) and finally by the $[0/90/\pm75]_S$ at 19.3 MPa (2800 psi). The damage initiation at the laminated composite structures started at different locations as shown in figure 3(a) and (b). At the $[0/90/\pm45]_S$ plies the fracture started at the middle stiffener, while at $[0/90/\pm\theta]_S$ for $\theta = 60°$ and 75° started at the laminate.

4.3 Collapse of the structure

After the fracture initiation happened, the cracks propagated rapidly and collapse of the

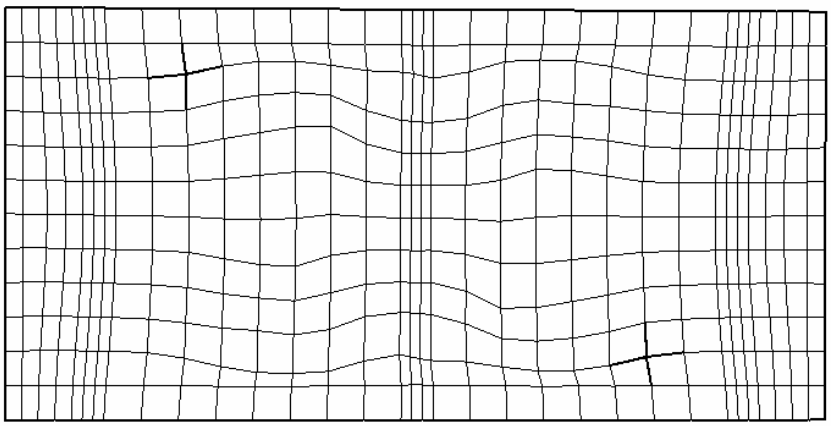

Figure 3(b). Fracture initiation at P = 19.3 MPa (2800 psi) [0/90/ ± 75]s S-Glass/Epoxy Stiffened plate.

structure occurs. First the structure with the $[0/90/\pm60]_S$ collapses at 26.38 MPa (3820 psi), follows the $[0/90/\pm45]_S$ at 27.44 MPa (3820 MPa) and finally the $0/90/\pm75]_S$ at 30 MPa (4351.1 psi), figure 2.

5. Conclusions

A computational simulation was used to evaluate the structural damage progression response of a S-Glass/epoxy $[0/90/\pm\theta]_S$ for θ = 45°, 60°, and 75° laminate fiber-reinforced composite structure under pressure. The conclusions follow:

Damage initiation started at low load level first at $[0/90/\pm45]_S$ and followed by the laminates $[0/90/\pm\theta]_S$ for θ = 60° and 75°. Matrix cracking due to transverse tensile failure mode occurred in all damaged plies. From the damaged plies, the percentage of the fiber fracture per laminate was 16 percent for the $[0/90/\pm45]_S$, 30 percent for the $[0/90/\pm60]_S$ and 33 percent for the $[0/90/\pm75]_S$, and happened at the bottom (0°) ply. In addition interply delamination took place at the top (0°) ply of the laminates with θ = 60° and 75°. Fracture through the thickness began at 91 percent ply damages, due to matrix cracking, fiber breaking and interply delamination. First fractured the laminate with θ = 45° at 15.168 MPa, followed by the laminate with θ = 60° at 16.96 MPa, and finally the laminate with θ = 75° at 19.3 MPa. After the damage initiation, the crack grew rapidly resulting in the collapse of the plate. The laminate configurations $[0/90/\pm\theta]_S$ for θ = 45°, 60°, 75° the optimum lay-up configuration is the $[0/90/\pm75]_S$, because it has the best damage tolerance with respect to the damage initiation and propagation to structural fracture.

Acknowledgment

The first author would like to thank the Research Committee of Technological Educational Institute of Serres, Greece, for funding this research project.

References

[1] Chamis C.C., P.L.N. Murthy, L. Minnetyan, (1996) Progressive fracture of polymer matrix composite structures, *Theoretical and Applied Fracture Mechanics* 25, 1–15.

[2] Huang, D., Minnetyan, L., (1998) Damage progression in carbon-fiber reinforced I-beams, ASCE Journal of Composites for Construction 2(1) 38–45.

[3] Sokolinsky, V.S., et al., (2007) Failure analysis of Space Shuttle reinforced carbon-carbon plates, International Journal of Computers & Structures, in the press.

[4] Gotsis, P.K.; Chamis, C.C., Minnetyan, L., (1995) Effect of Combined Loads in the Durability of a stiffened Adhesively Bonded Composite Structure. Proceedings of the 36th AIAA/ASME/ASCE/AHS/ASC Structures, Structural Dynamics, and Material Conference AIAA–95–1283–CP, part 2, 1083–1092.

[5] Chamis, C.C.; Gotsis, P.K. and Minnetyan, L., (1995) Damage Progression in Bolted Composite Structures, Proceedings of the USAF Structural Integrity Program Conference.

[6] Gotsis, P.K.; Chamis, C.C and Minnetyan, L. (1996) Progressive

Fracture of Fiber Composite Shell Structures Under Internal Pressure and Axial Loads, NASA TM-107234.

[7] Gotsis, P.K., Chamis, C.C., David, K. and Abdi F., (2007) Progressive Fracture of Laminated Fiber-Reinforced Composite Stiffened Plate under Thermo-mechanical Loads, IXth International conference on Mecomechanics MESO2007. Presquile de Giens, France, May 13–17.

[8] Gotsis, P.K., Chamis, C.C., Abdi, F., Tsouros, K., (2007) Progressive Fracture of Laminated Fiber-Reinforced Composite Stiffened Plate under Pressure, COMP-O7, 6th International Symposium on Advanced Composite Technologies. Corfu, Greece, May 16–18.

[9] Gotsis, P.K., Chamis, C.C., Tsouros, K. and David, K., (2007) Damage Progression of [0/90/±45]S Laminated Fiber-Reinforced Composite Stiffened Plate Under Mechanical Load, 8th International Congress on Mechanics. Patras, Greece, July 12–14.

[10] Murthy, P.L.N., Chamis, C.C., (1986) Integrated Composite Analyzer (ICAN): Users and Programmers Manual, NASA Technical Paper 2515.

[11] Nakazawa, S., Dias, J.B., Spiegel, M.S., (1987) MHOST Users's Manual, Prepared for NASA Lewis Research Center by MARC Analysis Research Corporation